R. & M. No. 3149
(20,222)
A.R.C. Technical Report

R. & M. No. 3149

MINISTRY OF AVIATION

AERONAUTICAL RESEARCH COUNCIL
REPORTS AND MEMORANDA

An Analysis of the Lateral-Directional Stability and Control of the Single-Rotor Helicopter

By G. F. LANGDON, B.Sc.(Eng.) and M. C. NEALE, M.Sc.(Eng.)

LONDON: HER MAJESTY'S STATIONERY OFFICE
1960
PRICE 11*s.* 0*d.* NET

An Analysis of the Lateral-Directional Stability and Control of the Single-Rotor Helicopter

By G. F. LANGDON, B.Sc.(Eng.) and M. C. NEALE, M.Sc.(Eng.)

COMMUNICATED BY THE DIRECTOR-GENERAL OF SCIENTIFIC RESEARCH (AIR), MINISTRY OF SUPPLY

*Reports and Memoranda No. 3149**

May, 1958

Summary. The lateral-directional stability of a single-rotor helicopter is investigated by solving the equations of motion for a typical aircraft. It is found that the motion has three constituent parts, two subsidences and an oscillation. The oscillation is slightly unstable at very low speeds but becomes more and more damped as the speed of the aircraft is increased. The response to disturbances of various kinds and to control movements is illustrated by means of examples. It is found that increasing altitude reduces the damping of the oscillatory motion and decreases the rolling effectiveness of the control. Flight measurements of the lateral-directional oscillation agree well with theory except for an overestimation of period at very low speeds.

Consideration is given to the effect of varying some design parameters; in particular it is shown that a large increase in roll damping at very low speeds will stabilise the lateral-directional oscillation and that a decrease in roll damping at high speed can lead to the appearance of a second oscillatory mode which may be unstable.

An Appendix shows the connection between certain stability derivatives and control positions in asymmetric flight.

1. *Introduction.* The lateral-directional stability of a single-rotor helicopter was investigated by Zbrozek in 1948[1]; since then there have been developments in rotor theory, notably the work of Amer on rotor damping[2]. Studies of some aspects of the lateral-directional motion have been made, but it was felt that for the interpretation of flight tests it would be useful to make a general investigation similar to those recently published for the longitudinal motion[3, 4].

The object of the present paper is to describe the lateral-directional characteristics of a single-rotor helicopter within the framework of classical stability theory as applied to aeroplanes.

For the sake of simplicity the rotor characteristics are calculated on the basis of uniform inflow with empirical corrections at low speeds based on full scale tests.

Sections 2 and 3 of this report detail the equations of motion and the general principles from which the stability derivatives are found and these apply to any helicopter configuration. The remainder of the paper is concerned with the application of these principles to a helicopter with a single lifting rotor, first considering the motion of a typical helicopter under various conditions and then proceeding to examine the effect of various changes in the basic parameters of the aircraft.

An Appendix shows that some of the stability derivatives can be found from measurements of control positions in steady asymmetric flight.

* Aeroplane and Armament Experimental Establishment report AAEE/Res/299, received 15th September, 1958.

Considerable use has been made of the methods developed in the study of aeroplane stability; in particular of the work of Melvill Jones[5].

2. *Equations of Motion.* The system of axes (based on Ref. 6) is shown in Fig. 1. The origin is at the centre of gravity of the aircraft. In the equilibrium condition the x axis is horizontal and forward and is fixed in the aircraft during the disturbed motion; the z axis is downward in the plane of symmetry of the aircraft and perpendicular to the x axis while the y axis is to starboard.

In the equilibrium condition the helicopter is moving with velocity V in the direction of the x axis (we have thus restricted the investigation to hovering and level flight). During a disturbance the helicopter has velocity v in the direction of the y axis and angular velocities p and r about the x and z axes in the directions shown in Fig. 1. It is assumed that the disturbances are small, so that their products can be neglected, and that the motion is entirely independent of any motion in the longitudinal plane.

Since v, p and r are small quantities we may write the force and moments acting on the aircraft in the form $Y = Y_e + Y_v v + Y_p p + Y_r r$, for example, where Y_e is the equilibrium value of Y and $Y_v = \partial Y/\partial v$, etc.

The equations of motion can then be written[7]

$$m\left(\frac{dv}{dt} + Vr - g\phi\right) = Y_v v + Y_p p + Y_r r + Y_{A1} A_1 + Y_{\theta t}\theta_t$$

$$A\frac{dp}{dt} - E\frac{dr}{dt} = L_v v + L_p p + L_r r + L_{A1} A_1 + L_{\theta t}\theta_t$$

$$C\frac{dr}{dt} - E\frac{dr}{dt} = N_v v + N_p p + N_r r + N_{A1} A_1 + N_{\theta t}\theta_t ,$$

where the last two terms in each equation represent the effect of control movements.

Adopting the system of non-dimensional notation of Ref. 8 and dividing the first equation by $As\,\rho\,(\Omega R)^2$ and the others by $As\,\rho\,(\Omega R)^2 R$ and replacing differentiation with respect to t by differentiation with respect to $\hat{t}$, the aerodynamic time, we have

$$\hat{v} - \hat{v}y_v - \frac{\dot{\phi}}{\mu_2}y_p + \left(\mu - \frac{y_r}{\mu_2}\right)\dot{\psi} - t_c'\phi = y_{A1}A_1 + y_{\theta t}\theta_t$$

$$-\hat{v}\frac{\mu_2 l_v}{i_a} + \ddot{\phi} - \dot{\phi}\frac{l_p}{i_a} - \ddot{\psi}\frac{i_e}{i_a} - \dot{\psi}\frac{l_r}{i_a} = \frac{\mu_2}{i_a}(l_{A1}A_1 + l_{\theta t}\theta_t)$$

$$-\hat{v}\frac{\mu_2 n_v}{i_c} - \ddot{\phi}\frac{i_e}{i_c} - \dot{\phi}\frac{n_p}{i_c} + \ddot{\psi} - \dot{\psi}\frac{n_r}{i_c} = \frac{\mu_2}{i_c}(n_{A1}A_1 + n_{\theta t}\theta_t) ,$$

where

$$\hat{v} = \frac{v}{\Omega R}; \qquad y_r = \frac{Y_r}{As\rho\Omega R^2}, \text{ etc.} \qquad i_c = \left(\frac{k_c}{R}\right)^2, \text{ etc.}$$

$$\mu_2 = \frac{m}{As\rho R}; \qquad l_v = \frac{L_v}{As\rho\Omega R^2}, \text{ etc.} \qquad \hat{t} = \frac{\Omega}{\mu_2}t$$

$$y_v = \frac{Y_v}{As\rho\Omega R}; \qquad l_r = \frac{L_r}{As\rho\Omega R^3}, \text{ etc.} \qquad t_c' = \frac{W}{As\rho(\Omega R)^2}$$

$$\dot{\psi} = \frac{d\psi}{d\tau}, \text{ etc.}$$

Assuming that ϕ, ψ and v are proportional to $e^{\lambda\tau}$ and expanding and rearranging the determinantal equation, we get a quintic for λ with one zero root. This zero root means that ψ is undetermined[7], or in other words that the aircraft has no preference for a particular compass heading. The motion then depends on the roots of $A\lambda^4 + B\lambda^3 + C\lambda^2 + D\lambda + E = 0$ where, from Ref. 8,

$$A = 1 - \frac{i_e^2}{i_a i_c}$$

$$B = -y_v\left(1 - \frac{i_e^2}{i_a i_c}\right) - \left(\frac{l_p}{i_a} + \frac{n_r}{i_c} + \frac{i_e n_p}{i_a i_c} + \frac{i_e l_r}{i_c i_a}\right)$$

$$C = y_v\left(\frac{l_p}{i_a} + \frac{n_r}{i_c} + \frac{i_e n_p}{i_e i_c} + \frac{i_e l_r}{i_c i_a}\right) + \left(\frac{l_p n_r}{i_a i_c} - \frac{l_r n_p}{i_a i_c}\right) + \frac{\mu_2 n_v}{i_c}\left(\mu_d - \frac{y_r}{\mu_2} - \frac{i_e y_p}{i_a \mu_2}\right)$$
$$+ \frac{\mu_2 l_v}{i_a}\left\{\frac{i_e}{i_c}\left(\mu_d - \frac{y_r}{\mu_2}\right) - \frac{y_p}{\mu_2}\right\}$$

$$D = -y_v\left(\frac{l_p n_r}{i_a i_c} - \frac{l_r n_p}{i_a i_c}\right) - \frac{\mu_2 n_v}{i_c}\left\{\frac{l_p}{i_a}\left(\mu_d - \frac{y_r}{\mu_2}\right) + \frac{l_r y_p}{i_a \mu_2} + \frac{i_e}{i_a} t_c'\right\}$$
$$+ \frac{\mu_2 l_v}{i_a}\left\{\frac{n_p}{i_c}\left(\mu_d - \frac{y_r}{\mu_2}\right) + \frac{n_r y_p}{i_c \mu_2} - t_c\right\}$$

$$E = \frac{t_c' \mu_2}{i_a i_c}(l_v n_r - n_v l_r).$$

3. *Method of Calculating the Derivatives.* Before the equations of motion can be solved the force and moment derivatives must be calculated.

Fig. 2 shows the type of rotor considered. It has flapping blades, the hinges of which are offset eR from its centre and its tip-path plane is tilted to port through an angle $(b_1 + A_1)$, b_1, the tilt of the tip-path plane relative to the control plane, being due to the variation in resultant airflow over each blade as it rotates and A_1, the tilt of the control plane, being due to the cyclic change in blade pitch caused by a sideways movement of the pilot's control.

The aerodynamic resultant force on the rotor is the thrust T, inclined to the control plane at an angle b' nearly, but not quite, equal to b_1. Due to the flapping hinge offset there is a rolling moment of $-F_c eR(b_1 + A_1)\sin^2\psi'$ for each blade which gives an average of $-\frac{1}{2}F_c eRb(b_1 + A_1)$ for the rotor. Now since there is no coupling with the longitudinal motion there is no variation in normal acceleration and T will remain constant during the disturbed motion so we have only to consider the variation of b_1 and b'.

It can be shown (Ref. 9, for example), that the effect of a sidewind is to tilt the rotor disc away from the direction of the sidewind and that the rotor disc tends to lag behind the fuselage during a rolling motion. These effects are expressed by the equations

$$\frac{\partial b_1}{\partial v} = \frac{8\theta}{3B} + \frac{2\lambda}{B^2} \qquad \text{(Refs. 1 and 9)}$$

$$\frac{\partial b'}{\partial \hat{v}} = \frac{\partial b_1}{\partial \hat{v}} + \frac{\delta B^2}{4t_c} \text{ since } \frac{\partial Y'/T}{\partial \hat{v}} \doteq \frac{\delta B^2}{4t_c}$$

$$\frac{\partial b_1}{\partial \hat{p}} = \frac{16}{\gamma \Omega B^4} \qquad \text{(Ref. 2)}$$

$$\frac{\partial b'}{\partial p} = \frac{\partial b_1}{\partial \hat{p}}\left(\frac{3}{2} - \frac{aB^3}{12}\frac{\theta}{t_c}\right) \qquad \text{(Ref. 2).}$$

When the helicopter is yawing about the z axis the rotational speed of the main rotor through the air is changed. This produces a damping moment given by $r(\partial Q/\partial r)$ or, expressed in non-dimensional terms, the part of n_r due to the effect is approximately $-2q_c$.

The effect of a yawing motion on a lifting rotor also depends on its distance from the centre of gravity, so that

$$\frac{\partial b_1}{\partial \hat{r}} = l\frac{\partial b_1}{\partial v},$$

$$\frac{\partial b}{\partial r} = l\frac{\partial b'}{\partial v}.$$

Sideslip will change the flow through a tail rotor and thus change its thrust. It can be shown that

$$\left(\frac{\partial t_c}{\partial \hat{v}}\right)_t = \left(\frac{-2B^2\alpha^3}{8\alpha^3 + as\alpha^2 - \dfrac{4st_c}{B^2}}\right)_t,$$

which reduces to

$$\left(\frac{\partial t_c}{\partial \hat{v}}\right)_t = \left(\frac{-2B^2a\,|\,\lambda\,|}{16\lambda + as}\right)_t \qquad \text{when hovering}$$

and to

$$\left(\frac{\partial t_c}{\partial \hat{v}}\right)_t = \left(\frac{-2B^2a\mu}{8\mu + as}\right)_t \qquad \text{at high speed (Ref. 4).}$$

The effect of roll and yaw on the tail rotor then follow from the geometry of the helicopter.

4. *Expressions for the Derivatives for a Helicopter with a Single Lifting Rotor.* The expressions which follow can be derived directly from Figs. 2 and 3. In each case (except for the control movement derivatives), the expression consists of two parts, the first due to the main rotor and the second to the tail rotor. The effect of the fuselage and any fixed surfaces can be calculated as for an aeroplane. We then have

$$y_v = -t_c\frac{\partial b'}{\partial \hat{v}} + \bar{D}\left(\frac{\partial t_c}{\partial \hat{v}}\right)_t$$

$$y_r = -t_c l\frac{\partial b'}{\partial \hat{v}} - \bar{D}l_t\left(\frac{\partial t_c}{\partial \hat{v}}\right)_t$$

$$y_p = -t_c\frac{\partial b'}{\partial \hat{p}} + \bar{D}h_t\left(\frac{\partial t_c}{\partial \hat{v}}\right)_t$$

$$y_{\theta t} = \bar{D}\left(\frac{\partial t_c}{\partial \theta}\right)_t$$

$$y_{A1} = -t_c$$

$$n_v = -t_c l\frac{\partial b'}{\partial \hat{v}} - \bar{D}l_t\left(\frac{\partial t_c}{\partial \hat{v}}\right)_t$$

$$n_r = -2q_c - t_c l^2\frac{\partial b'}{\partial \hat{v}} - \bar{D}l_t^2\left(\frac{\partial t_c}{\partial \hat{v}}\right)$$

$$n_p = -t_c l\frac{\partial b'}{\partial \hat{p}} + \bar{D}l_t h_t\left(\frac{\partial t_c}{\partial \hat{v}}\right)$$

$$n_{\theta t} = -\bar{D}\left(\frac{\partial t_c}{\partial \theta}\right)_t$$

$$n_{A1} = t_c l$$

$$l_v = -t_c\left(h + \frac{f_c}{t_c}\frac{be}{2}\frac{db_1}{db}\right)\frac{\partial b'}{d\hat{v}} + \bar{D}h_t\left(\frac{\partial t_c}{\partial \hat{v}}\right)$$

$$l_r = -t_c l\left(h + \frac{f_c}{t_c}\frac{be}{2}\frac{db_1}{db'}\right)\frac{\partial b'}{\partial \hat{v}} - \bar{D}l_t h_t\left(\frac{\partial t_c}{\partial \hat{v}}\right)_t$$

$$l_p = -t_c\left(h + \frac{f_c}{t_c}\frac{be}{2}\frac{db_1}{db'}\right)\frac{\partial b'}{\partial p} + \bar{D}h_t{}^2\left(\frac{\partial t_c}{\partial \hat{v}}\right)_t$$

$$l_{\theta t} = \bar{D}h_t\left(\frac{\partial t_c}{\partial \theta}\right)_t$$

$$l_{A1} = -t_c\left(h + \frac{f_c}{t_c}\frac{be}{2}\right)$$

where $\bar{D}$, the tail thrust ratio, equals $\{As(\Omega R)^2\rho\}_t/\{As(\Omega R)^2\rho\}$.
h, h_t, l and l_t are all measured with respect to the x and z axis, not the fuselage datum and for a given helicopter will vary with fuselage attitude. In particular l will always be small and h_t may change considerably with airspeed.

5. *Solution of the Equations for a Typical Helicopter.* 5.1. *Values of the Derivatives.* Numerical values for the derivatives have been calculated for a *Sycamore*, the relevant particulars of which are given in Table 1. At low speeds the value of B, the tip-loss factor, was taken from the full-scale results of Ref. 10.

Calculations were made (*a*) assuming that the fuselage attitude remained constant throughout the speed range and (*b*) using the actual fuselage attitude as recorded in flight tests; the results are shown in Fig. 4.

5.2. *Examination of the Quartic for* λ. Before considering solutions of the equations of motion it is interesting to examine the form of the quartic for λ. The coefficients of this are plotted in Fig. 5. To see more clearly the reason for the change in C and D with tip-speed ratio it is useful to retain only the dominant terms in the expressions for the coefficients. We then have

$$A = 1$$

$$B = -\left(\frac{l_p}{i_a} + \frac{n_r}{i_c}\right)$$

$$C = \frac{l_p n_r}{i_a i_c} + \frac{n_v \mu_2}{i_c}\mu$$

$$D = -t_c\frac{\mu_2 l_v}{i} + \frac{\mu_2}{i_a i_c}(n_v l_p)\mu$$

$$E = \frac{t_c \mu_2}{i_a i_c}(l_v n_r - n_v l_r).$$

From Fig. 5 it can be seen that all the coefficients of the quartic are positive throughout the speed range, and there can therefore be no purely divergent motion. For complete stability it is necessary (Ref. 7, for example) for Routh's discriminant $BCD - B^2E - D^2$ to be positive and from Fig. 5 we see that this condition is fulfilled except at very low values of μ where the discriminant is negative and there will be an unstable oscillation.

5.3. *Numerical Solution of the Quartic.* We find that there are two real roots of the equation. The first is a negative real root approximately equal to $-B$ at low values of μ and decreasing numerically as μ increases. This corresponds to a motion which rapidly dies away, decaying to half its original value in about 0·36 sec at $\mu = 0$ and 1·09 sec at $\mu = 0{\cdot}25$.

The second real root is approximately equal to $-E/D$ which corresponds to another decaying motion, falling to half its original value in about 2·1 sec at $\mu = 0$ or 7 sec at $\mu = 0{\cdot}25$.

There remains a pair of complex roots which correspond to an oscillation with period varying from about 10 sec at $\mu = 0$ to 2·5 sec at $\mu = 0{\cdot}25$. The motion is slightly unstable at $\mu = 0$, having time to double amplitude of about 16·7 sec, but becomes increasingly stable as μ is increased above about 0·025 the time to half amplitude being 0·95 sec at $\mu = 0{\cdot}25$.

Fig. 6 shows the roots of the quartic in non-dimensional form.

5.4. *Flight Measurements of the Lateral-Directional Oscillation.* The predicted values of the period and damping of the oscillation for a *Sycamore* are shown in Fig. 7 together with the results of flight tests. It can be seen that the theory agrees quite well with the experimental values of the damping factor but that at low speeds the period of the motion is much less than the predicted value. The aircraft was destroyed in an accident before more low-speed results could be obtained.

5.5. *Response to a Disturbance.* The way in which the different modes combine to give the complete motion of the helicopter following a disturbance is shown by the theoretical curves of Fig. 8, obtained by solving the equations of motion on an analogue computer. The examples chosen show the response of the aircraft to sudden disturbances in roll, yaw and sideslip while hovering and while in level flight at 56 kt.

It must be remembered that in making these calculations we are straining somewhat the assumption of small deviations from straight and level flight. It is also worth pointing out that, at least in the final stages of the motions to be described, the thrust on a real rotor would change so that the later part of the theoretical motion may not be apparent in practice.

It can be seen that the oscillation predominates in the hovering case, the motion consisting of a slowly increasing oscillation like a falling leaf with the aircraft also yawing about a heading different to the original. The new mean heading is reached after about eight sec, this motion corresponding to the numerically smaller real root, and the remaining aperiodic mode decays too rapidly to be obvious on the diagrams. Flight tests show that the motion is very much as predicted although the period is less, as mentioned earlier. In practice it is difficult to prevent a longitudinal oscillation developing at low speeds.

The diagrams illustrating the response of the helicopter to the same disturbances while flying at 56 kt ($\mu = 0{\cdot}15$) show that the motion is now of a quite different character and in particular that the oscillation, in which sideslip and yaw now predominate, is much less important, being so damped that it dies out after seven or eight sec. The numerically larger real root is evident during the first two sec or so after which the smaller root leads to a slow return to steady flight on a new heading after about 15 sec.

Again, flight tests confirm that the motion is generally as shown, but it is difficult to prevent the longitudinal motion intruding during the later stages.

5.6. *Response to Controls.* Fig. 9 shows the theoretical motion of a *Sycamore* following instantaneous control inputs, calculated using an analogue computer. In practice, of course, manoeuvres are made by the co-ordinated use of both cyclic pitch and tail rotor controls but it is convenient to consider the response of the aircraft to each control applied separately.

Turning first to the effect of a lateral control step we see that in hovering the motion is dominated by the unstable oscillations, as might be expected.

At 30 kt the aircraft is stable and hardly any oscillation is excited by the applied rolling moment. As soon as the stick is moved sideways, to the right, for example, the helicopter begins to roll at an increasing rate; the high value of $(-l_p)$ due to the fact that the main rotor thrust vector tends to lag behind the fuselage tends to damp the motion and a maximum rate of roll of about $2\frac{1}{2}$ deg/sec is reached after about 1 sec. The sideways tilt of the disc causes right sideslip; both sideslip and roll act on the tail rotor so that the aircraft turns to the right (since n_v and n_p are both positive).

The effect of increasing speed is shown by the response diagrams at 50 and 80 kt. The main change is due to the marked decrease in $(-l_p)$ with speed which causes an increase in the maximum rate of roll and gives the effect of more sensitive controls.

Considering now the response to a sudden 1-deg change in tail rotor pitch, we see first that at $\mu = 0$ the motion is once more primarily an unstable oscillation, this time superimposed on a rate of turn of about 12 deg/sec. The response curves at forward speed show that the oscillation is more marked by a change in tail rotor pitch than by lateral cyclic. The immediate effect of the application of 'rudder' to the right, for example, is to start the helicopter turning to the right, sideslipping to the left and, since the tail rotor is above the centre of gravity, rolling to the left. The rate of turn is damped by the tail rotor (n_r is negative) and quickly reaches its peak after which it oscillates before settling down to a steady value while the sideslip is damped by its effect on both the main and tail rotors (y_v is negative) and it, too, reaches a final value as the oscillation dies away. The initial roll to the left is opposed by the effect of the left sideslip on both rotors (l_v is negative) and the roll angle soon reverses and tends toward a final steady right bank. The effect of the changes with speed can be seen by comparing the diagrams for 30, 50 and 80 kt. The initial peaks of rate of turn, sideslip and roll are reduced as n_r, y_v and l_v become numerically larger, though the situation is complicated by the fact that $(-y_p)$, which affects the initial peak of sideslip and $(-l_p)$, which affects the initial peak of roll, decrease numerically with speed.

It is found that the changes in the final rate of turn and angle of bank shown in Fig. 9 are mainly due to the variation with speed of l_v and n_v. An increase in n_v results in an increase in the turning moment opposing the motion due to sideslip and an increase in $-l_v$ increases the rolling moment, assisting the motion due to sideslip, so that broadly speaking, it can be expected that an increase in $-n_v/l_v$ will decrease the final rate of turn and angle of bank. Fig. 10 shows $-n_v/l_v$ for a *Sycamore* and it can be seen that this ratio increases from $\mu = 0$ to $\mu = 0{\cdot}11$ after which it becomes smaller. This accounts for the final value of bank and rate of turn being lower at 50 kt than at either 30 or 80 kt.

5.6. *The Effect of Change in Altitude.* When discussing an aeroplane it is possible to demonstrate the effect of a change in air density by changing μ_2, the relative density parameter, and considering the motion at various altitudes at the same lift coefficient. With a helicopter the situation is rather more complicated: firstly, because for a given helicopter the thrust coefficient will increase with

altitude as the operating range of rotor speed is usually small; secondly, because air density enters directly into Lock's inertia number, γ.

As an illustration of the effect of altitude, calculations have been made for a *Sycamore* at a tip-speed ratio of 0·15 from sea level to 15,000 ft at constant weight and rotor speed. Most of the derivatives change with t_c, the changes are less than 30 per cent with the exception of l_p which, depending on both t_c and γ, has double its sea-level value at 15,000 ft. Fig. 11 shows the period and damping of the lateral oscillation, and it can be seen that at greater heights the damping is reduced appreciably and the period becomes slightly longer.

The change with altitude in the response to lateral cyclic pitch is shown in Fig. 12. Due mainly to the increase of l_p with decreasing density the maximum rate of roll for a given control movement becomes smaller as the height increases; this means that the helicopter takes longer to reach a given angle of bank and leads to a feeling of 'lag' in the controls. The response to changes of tail-rotor pitch is not greatly affected by altitude.

6. *The Effect of Changing Various Parameters on the Solution for a Typical Helicopter.* In the following sub-sections an investigation is made into the effect of changing various parameters in turn, retaining the basic rotor system.

The results are presented in terms of real time. Conversion to the non-dimensional time scale may be made by dividing the time in seconds by $t_c \, \Omega \, R/g \; (= \mu_2 \, \Omega)$. This conversion factor is 1·17.

6.1. *The Effect of Increased Damping in Roll or Yaw on the Lateral Directional Oscillation in the Hovering Case.* The negative value of Routh's discriminant at low tip-speed ratios is caused by the decrease in C and D as the tip-speed ratio becomes small. This is due to the Vr term in the first equation of motion and is a dynamic rather than an aerodynamic effect, so that small design changes will not change the basic shape of the C and D curves in Fig. 5.

It is found that the most promising method of stabilising the oscillation is to increase the damping in roll $(-l_p)$, the damping in yaw $(-n_r)$ or both. The roll damping must be more than doubled or the damping in yaw multiplied by three to achieve stability; the use of large flapping hinge offsets might give the required l_p.

6.2. *The Effect of Reduced Roll Damping at High Tip-Speeds.* The damping in roll $(-l_p)$ decreases with increasing tip-speed ratio and it was pointed out by Amer in Ref. 2 that the damping may even become negative for powerful high-speed helicopters. To investigate this, calculations were made on an analogue computer using as a starting point the equations of motion for a *Sycamore* with $\mu = 0{\cdot}25$ and reducing $(-l_p)$ in stages.

The results are shown in Fig. 13. It can be seen the reduction in roll damping leads first to an increased sensitivity to disturbances coupled with a quicker subsidence to the trimmed condition. This corresponds to a numerical decrease in the 'large' real root and a numerical increase in the 'small' real root consequent on the reduction of the coefficients C and D respectively. As $-l_p$ is further reduced below about 0·006 these two roots combine to give a damped oscillation with a period of about 20 sec and if $-l_p$ is made smaller then about 0·001 the oscillation becomes unstable.

We see then that there is a possibility that for helicopters with low damping in roll at high speeds the disturbed motion may consist of two oscillations: one of period of the order of two sec which will probably be quite heavily damped and one of period of the order of 20 sec which may be unstable.

Physically $-l_p$ could be reduced by decreasing the flapping hinge offset or increasing the inertia number of the rotor.

6.3. *The Effect of Tail-Thrust Ratio and of Tail-Rotor Position on the Lateral-directional Oscillation in Cruising Flight.* The influence of the tail rotor is governed by three parameters: $\bar{D}$, the tail thrust ratio; l_t, a measure of its distance behind the aircraft centre of gravity, and h_t, which defines its distance above the aircraft centre of gravity.

It is found that variation in h_t has little effect on the oscillatory motion in cruising flight. The results of changes in $\bar{D}$ and l_t are shown in Figs. 14 and 15 and are, as might be expected, an increase in either $\bar{D}$ or l_t leading to increased damping and a shorter period. The numerical results shown in Figs. 14 and 15 are approximate, because the calculations were made assuming a constant value of $(\partial t_c/\partial \hat{v})_t$ which will in fact change slightly with the characteristics of the tail rotor and with the change of tail-rotor thrust consequent on the change of l_t.

6.4. *The Effect of Changing l_v and n_v.* The derivatives l_v and n_v, which may be interpreted as 'effective dihedral' and 'weathercock stability' respectively, are of interest for two reasons: first, because they are relatively easy to alter by the addition of fixed surfaces to the fuselage (except at very low speeds) and second, because it is easy to establish their signs, and possible to measure their values, by means of steady flight tests as shown in the Appendix.

We first consider the effect of wide changes in the derivatives on the lateral-directional oscillation at a moderate speed ($\mu = 0{\cdot}15$). The results are shown in Fig. 16, from which it can be seen that a reduction in n_v is destabilising while a reduction in the numerical value of l_v increases the stability, the period in each case increasing as the damping falls.

To see more fully the effect of changes in l_v and n_v on the stability of the motion, refer to Fig. 17. This shows the region of the l_v, n_v plane within which the motion of the helicopter will be completely stable, the region being bounded on the one side by the line $E = 0$, which denotes neutral stability of the slowly developing motion corresponding to the small real root of the stability quartic and on the other side by the line representing neutral stability of the lateral-directional oscillation. The values of l_v and n_v for a *Sycamore* are shown on each diagram.

7. *Discussion and Conclusion.* The lateral-directional stability of a helicopter has been illustrated by the solution of the equations of motion for a particular helicopter. It was found that the motion consists of three modes: two subsidences and an oscillation. The oscillation is unstable when the aircraft is hovering or flying at very low forward speeds but as the forward speed increases the oscillatory mode becomes more and more heavily damped. Its period varies from about 6 sec in hovering to 2 sec at high speed. Of the two subsidences one decays to half its value in about one third of a second at low speed and its damping decreases as the speed becomes greater; the other represents a motion which decays much more slowly, taking roughly 6 sec to reach half its original value.

The main effect of altitude is a decrease in the apparent lateral control power, *i.e.*, a given control movement may produce a roll angle of 10 deg in 4 sec at sea level and take $7\frac{1}{2}$ sec to produce the same result at 10,000 ft.

It is theoretically possible to make the oscillation stable when hovering by much increasing the value of roll damping, possibly by using large flapping hinge offsets. The damping in roll decreases markedly at high speeds and there is a possibility of this causing the two subsidences to combine to give a second oscillation which, with very small values of roll damping, would become unstable. The analysis is being extended to cover tandem-rotor helicopters.

Acknowledgement. Acknowledgement is due to R. W. Coombes who carried out a large part of the computation involved in the preparation of this report.

LIST OF SYMBOLS

A		Disc area; coefficient of λ^4 in non-dimensional quartic
A_1		Lateral cyclic pitch applied by control; positive to the left
a		Slope of blade lift coefficient/incidence curve
B		Tip-loss factor; coefficient of λ^3 in non-dimensional quartic
b		Number of blades
b'		Sideways inclination of thrust vector to control plane; positive to the left
b_1		Sideways tilt of rotor disc relative to control plane; positive to the left
C		Coefficient of λ^2 in non-dimensional quartic
c		Mean chord of blade
D		Coefficient of λ in non-dimensional quartic
$\bar{D}$		Tail thrust ratio $= \{As(\Omega R)^2\rho\}_t/\{As(\Omega R)^2\rho\}$
E		Constant term in non-dimensional quartic
e		Flapping hinge offset divided by R
F_c		Centrifugal force on one blade
f_c	$=$	$F_c/\rho sA\,(\Omega R)^2$
g		Gravitational acceleration
h		Distance of c.g. below rotor hub divided by R
h_t		Distance of tail-rotor centre above c.g. divided by R
i_a		Moment of inertia of helicopter about rolling axis divided by mR^2
i_c		Moment of inertia of helicopter about yawing axis divided by mR^2
i_e		Product of inertia of helicopter about rolling and yawing axes divided by mR^2
I_b		Moment of inertia of rotor blade about flapping hinge
L		Rolling moment, positive 'right wing down'
L_{A1}	$=$	$\partial L/\partial A_1$
L_p	$=$	$\partial L/\partial p$
L_r	$=$	$\partial L/\partial r$
L_v	$=$	$\partial L/\partial v$
$L_{\theta t}$	$=$	$\partial L/\partial \theta_t$
l		Distance of c.g. behind rotor centre divided by R
l_{A1}	$=$	$L_{A1}/\rho sA(\Omega R)^2\,R$
l_p	$=$	$L_p/\rho sA\Omega R^3$
l_r	$=$	$L_r/\rho sA\Omega R^3$
l_t		Distance of centre of tail rotor behind c.g., divided by R
l_v	$=$	$L_v/\rho sA\Omega R^2$
$l_{\theta t}$	$=$	$L_{\theta t}/\rho sA(\Omega R)^2 R$
m		Mass of helicopter
N		Yawing moment; positive for right turn
N_{A1}	$=$	$\partial N/\partial A_1$
N_p	$=$	$\partial N/\partial p$
N_r	$=$	$\partial N/\partial r$
N_v	$=$	$\partial N/\partial v$
$N_{\theta t}$	$=$	$\partial N/\partial \theta_t$

n_{A1}	=	$N_{A1}/\rho s A(\Omega R)^2 R$
n_p	=	$N_p/\rho s A(\Omega R)^2$
n_r	=	$N_r/\rho s A(\Omega R)^2$
n_v	=	$N_v/\rho s A \Omega R^2$
$n_{\theta t}$	=	$N_{\theta t}/\rho s A(\Omega R)^2 R$
p		Rolling velocity; positive 'right wing down'
$\hat{p}$	=	p/Ω
Q		Torque on main rotor
q_c	=	$Q/As\rho(\Omega R)^2 R$
R		Rotor radius
r		Yawing velocity; positive for right turn
$\hat{r}$	=	r/Ω
s		Rotor solidity $bc/\pi R$
T		Rotor thrust
t		Time, or as a suffix signifying 'tail rotor'
$\hat{t}$		Aerodynamic time
t_c	=	$T/As\rho(\Omega R)^2$
t_c'	=	$W/As\rho(\Omega R)^2$
V		Helicopter speed
v		Sideslip velocity; positive for sideslip to the right
$\hat{v}$	=	$v/\Omega R$
$\dot{\hat{v}}$	=	$d\dot{v}/d\hat{t}$
W		Weight of helicopter
X		Force in the direction of x axis (Fig. 1)
Y		Force in the direction of y axis (Fig. 1)
Y'		Lateral force on rotor parallel to tip-path plane
Y_{A1}	=	$\partial Y/\partial A_1$
Y_p	=	$\partial Y/\partial p$
Y_r	=	$\partial Y/\partial r$
Y_v	=	$\partial Y/\partial v$
$Y_{\theta t}$	=	$\partial Y/\partial \theta_t$
y_{A1}	=	$Y_{A1}/\rho s A(\Omega R)^2$
y_p	=	$Y_p/\rho s A \Omega R^2$
y_r	=	$Y_r/\rho s A \Omega R^2$
y_v	=	$Y_v/\rho s A \Omega R$
$y_{\theta t}$	=	$Y_{\theta t}/\rho s A(\Omega R)^2$
α	=	$\sqrt{(\mu_d^2 + \lambda^2)}$
δ		Blade mean profile-drag coefficient
γ		Lock's inertia number, $\rho a c R^4/I_b$
θ		Collective pitch on main rotor
θ_t		Collective pitch of tail rotor
λ		Inflow parameter = (flow up through the disc)/ΩR, or root of non-dimensional stability quartic
λ_1		Root of stability quartic expressed in real time

μ		Tip-speed ratio $V \cos \alpha / \Omega R$
μ_2		Relative density parameter $m/\rho s A R$
ρ		Air density
τ	$=$	$t/\hat{t} = \mu_2/\Omega$
ϕ		Angle of bank; positive 'right wing down'
$\dot{\phi}$	$=$	$d\phi/d\hat{t}\ (\equiv p)$
$\ddot{\phi}$	$=$	$d^2\phi/d\hat{t}^2\ (\equiv dp/d\hat{t})$
ψ		Angle of yaw; positive for nose to right
ψ'		Angle of rotation of blade (Section 3)
$\dot{\psi}$	$=$	$d\psi/d\hat{t}\ (\equiv r)$
$\ddot{\psi}$	$=$	$d^2\psi/d\hat{t}^2\ (\equiv dr/d\hat{t})$
Ω		Rotor rotational speed

REFERENCES

No.	*Author*	*Title, etc.*
1	J. Zbrozek	Investigation into the lateral and directional behaviour of a single rotor helicopter. R. & M. 2509. June, 1948.
2	K. B. Amer	Theory of helicopter damping in pitch and roll and a comparison with flight measurements. N.A.C.A. Tech. Note 2136. October, 1950.
3	F. O'Hara	An analysis of the longitudinal stability and control of a single-rotor helicopter. R. & M. 2958. July, 1954.
4	A. R. S. Bramwell	Longitudinal stability and control of the single-rotor helicopter. R. & M. 3104. January, 1957.
5	M. B. Jones .. .. .. W. F. Durand (editor)	*Dynamics of the Airplane. Division N of Aerodynamic Theory.* Julius Springer, Berlin. 1935.
6	L. W. Bryant and S. B. Gates ..	Nomenclature for stability coefficients. R. & M. 1801. October, 1937.
7	W. J. Duncan	*Control and Stability of Aircraft.* Cambridge University Press. 1952.
8	A. Armitage	Notations for rotorcraft work. C.P. 314. April, 1956.
9	A. A. Nikolsky	*Helicopter Analysis.* John Wiley and Sons, Inc. New York. 1951.
10	A. L. Oliver	The low-speed performance of a helicopter. C.P. 112. May, 1952.
11	H. J. Van der Mass	Lateral and directional control and the measurement of aerodynamic coefficients in steady asymmetric flight and in flight on asymmetric power. A.G.A.R.D. Flight Test Manual. Vol. II. Chap. 5.

TABLE 1

Leading Particulars of Sycamore used in Calculations

t_c	=	0·0516	at sea level
$\frac{1}{2}f_c b_e$	=	0·00380	at sea level
μ_2	=	31	at sea level
$\overline{D}$	=	0·0512	
γ	=	9·34 at sea level	
i_c	=	0·0655	
i_a	=	0·0133	
i_e	=	0	
h	=	0·174	
l_t	=	1·33	
l			See Fig. 18
h_t			See Fig. 18

APPENDIX

Control Positions in Steady Asymmetric Flight

1. *General.* In this Appendix we show that the signs of l_v, n_v and the coefficient E of the stability quartic can be found from measurements of control positions in steady asymmetric flight. The values of l_v and n_v can be found from the same data if the control derivatives l_{A1}, $l_{\theta t}$ and $n_{\theta t}$ are accurately known.

The method of analysis is taken from Ref. 11 with the slight adaptations necessary for its application to a helicopter instead of an aeroplane.

2. *Equations of Motion.* In steady flight the equations of motion become

$$\hat{v}l_v + \frac{lr}{\mu_2}\dot{\psi} + l_{A1}A_1 + l_{\theta t}\theta_t = 0 \tag{1}$$

$$\hat{v}n_v + \frac{n_r}{\mu_2}\dot{\psi} + n_{A1}A_1 + n_{\theta t}\theta_t = 0\,. \tag{2}$$

3. *Steady Yawed Flight.* In this case we have $\dot{\psi} = 0$ and thus

$$l_v = -\,l_{A1}\frac{dA_1}{d\hat{v}} - l_{\theta t}\frac{d\theta_t}{d\hat{v}} \tag{3}$$

$$n_v = -\,n_{\theta t}\frac{d\theta_t}{d\hat{v}} - n_{A1}\frac{dA_1}{d\hat{v}}\,. \tag{4}$$

Now l_{A1} and $n_{\theta t}$ are always negative, $l_{\theta t}$ is positive and n_{A1} can be neglected so that we have from (3) that l_v is negative (positive effective dihedral) if

$$\left\{\frac{dA_1}{d\hat{v}} + \frac{l_{\theta t}}{l_{A1}}\left(\frac{d\theta_t}{d\hat{v}}\right)\right\} \text{ is negative.}$$

This will always be so if $dA_1/d\hat{v}$ is negative and $d\theta_t/d\hat{v}$ is positive.

Likewise from (4) n_v is positive (positive weathercock stability) if $d\theta_t/d\hat{v}$ is positive, remembering that the sign convention is such that positive sideslip means flight with the nose of the aircraft to the left of the flight path, positive A_1 means that the stick is moved to the left and positive θ_t means that the left pedal is pushed forwards.

It is, of course, possible to calculate the values of l_v and n_v as well as their signs but this depends on the accuracy with which the values of the control parameters l_{A1}, $l_{\theta t}$ and $n_{\theta t}$ are known.

4. *Steady Turns on Cyclic Control Only.* Eliminating $\hat{v}$ from (1) by (2) and rearranging with $\theta_t = 0$ we have

$$\frac{l_v n_r - n_v l_r}{n_v \mu_2} = l_{A1}\left(1 - \frac{n_{A1}\, l_v}{l_{A1}\, n_v}\right)\frac{dA_1}{d\dot{\psi}},$$

and since mA_1/lA_1 can be neglected, we say that E will be positive if $dA_1/d\dot{\psi}$ is negative and n_v is positive.

5. *Flight Test Results from Steady Yawed Flight.* Flight measurements made during preliminary tests on a *Sycamore* are shown in Fig. 19 to illustrate the method rather than as accurate results. It can be seen that $dA_1/d\hat{v}$ is negative and $d\theta_t/d\hat{v}$ is positive, so that the aircraft has both positive dihedral effect and weathercock stability.

To obtain these results the helicopter was fitted with a yaw-meter and continuous trace recorders for control positions and yaw. The position error of the air-speed measuring system was first checked in yawed flight by flying in formation with another helicopter, after which the aircraft was flown at constant equivalent air speed at various angles of yaw and the stick and pedal position recorded.

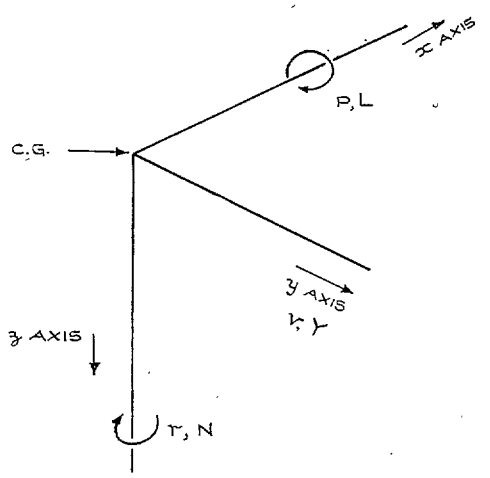

FIG. 1. Axes.

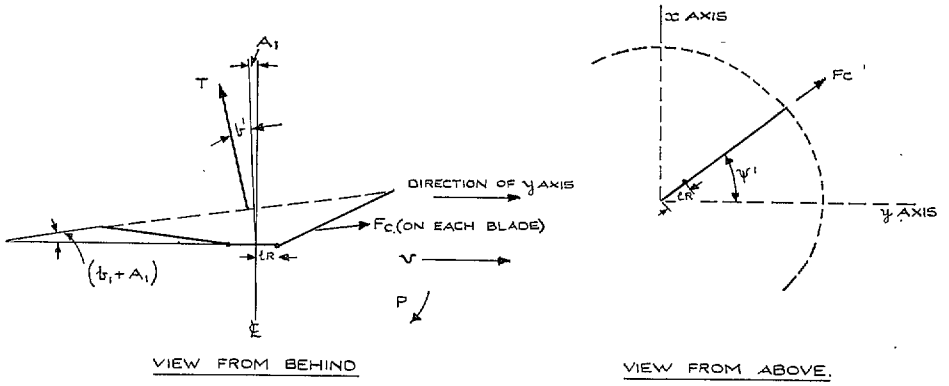

FIG. 2. Forces on rotor.

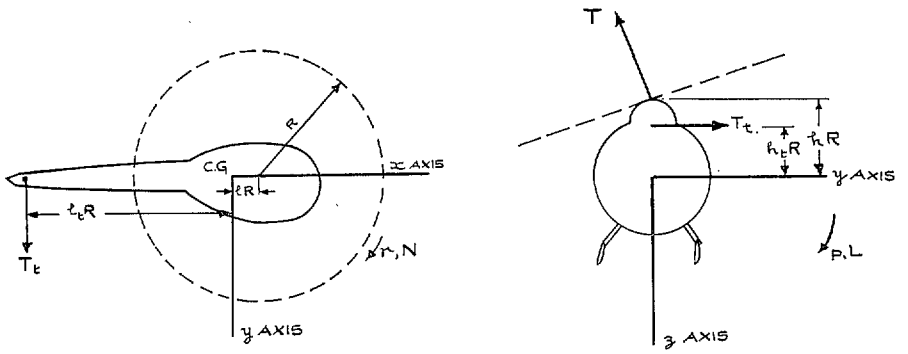

FIG. 3. Lay-out of single-rotor helicopter.

FULL LINE – FUSELAGE ATTITUDE
FROM FLIGHT TEST
DASHED LINE – FUSELAGE LEVEL.

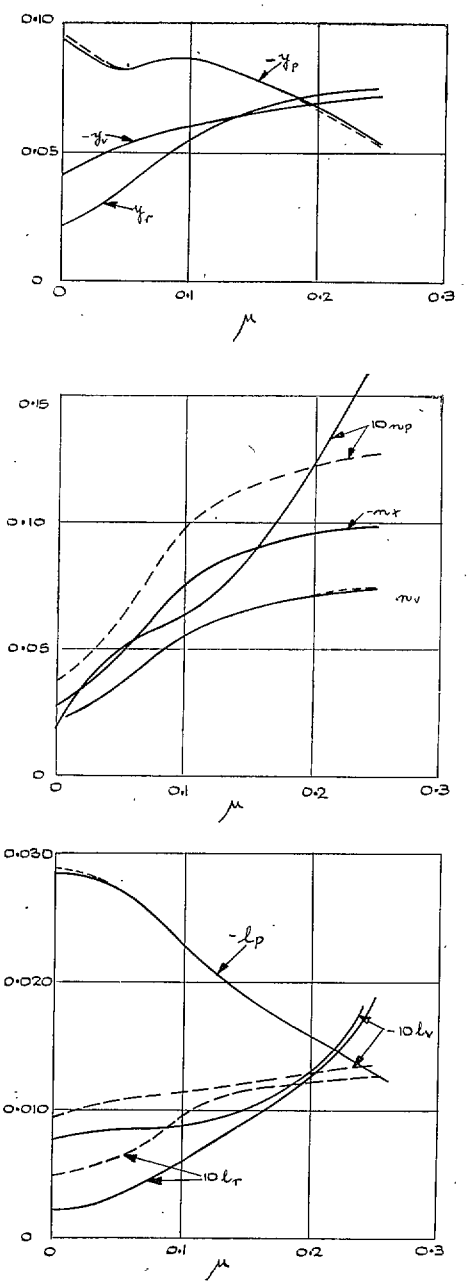

FIG. 4. Lateral-directional stability derivatives for a *Sycamore* at 2,000 ft I.C.A.N.

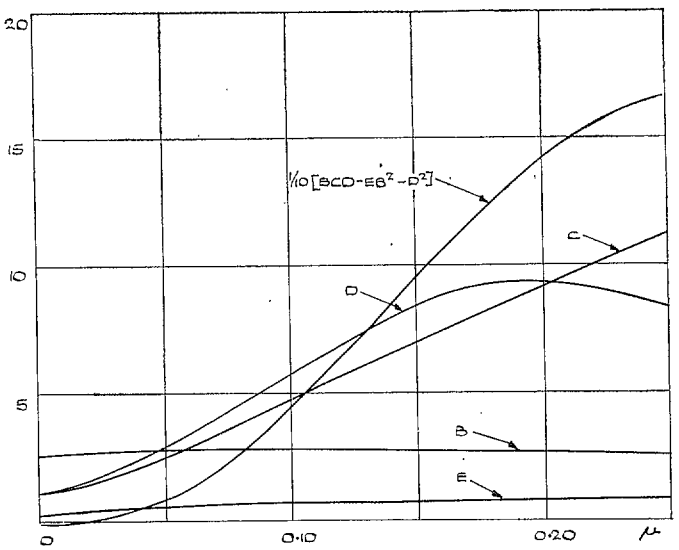

FIG. 5. Coefficients of non-dimensional stability quartic and Routh's discriminant for a *Sycamore*.

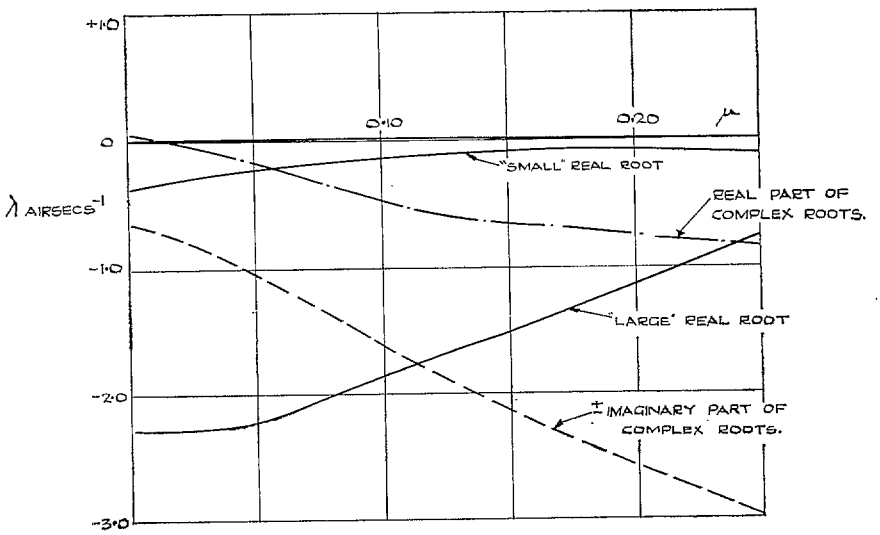

FIG. 6. Roots of non-dimensional stability quartic for a *Sycamore*.

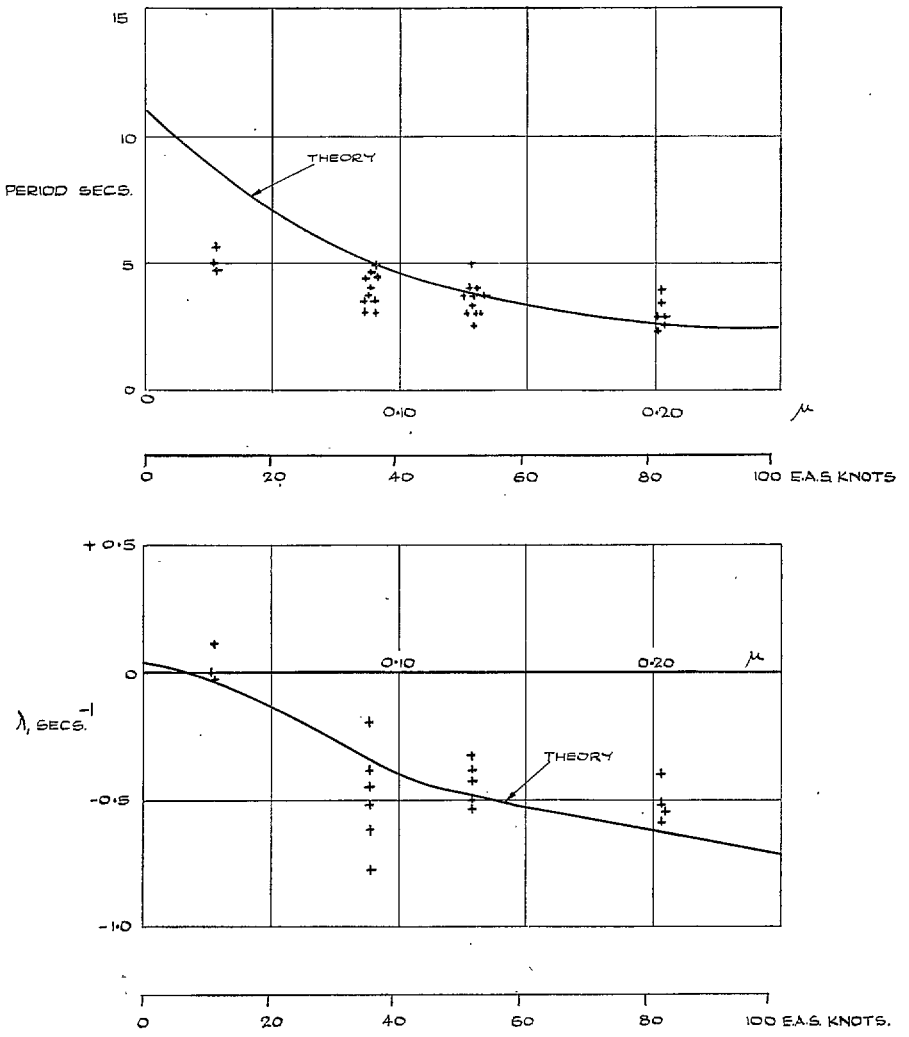

FIG. 7. Period and damping of lateral-directional oscillation. Comparison with experiment for *Sycamore* at 2,000 ft I.C.A.N.

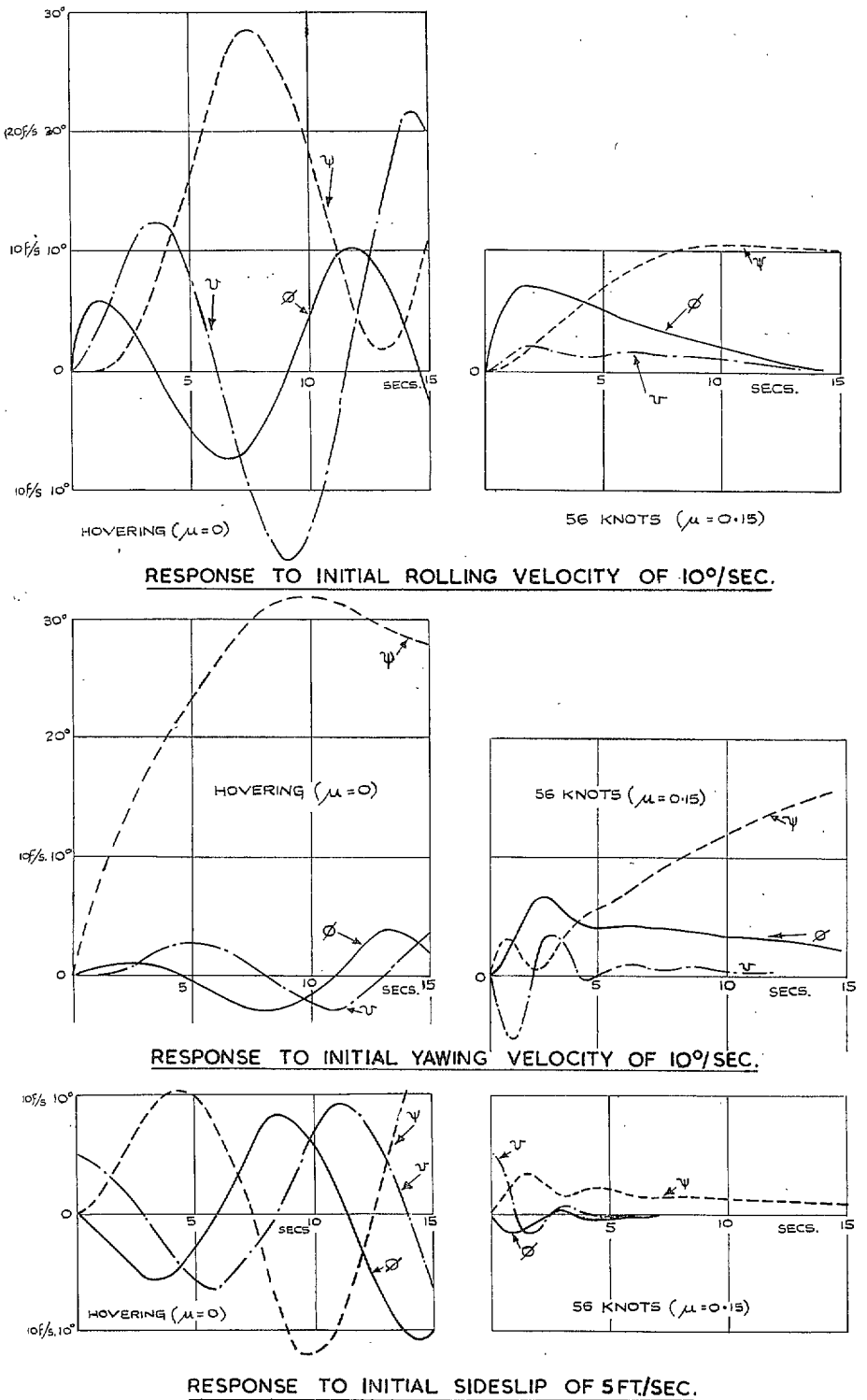

FIG. 8. Theoretical response of *Sycamore* to disturbances while hovering and at 56 kt.

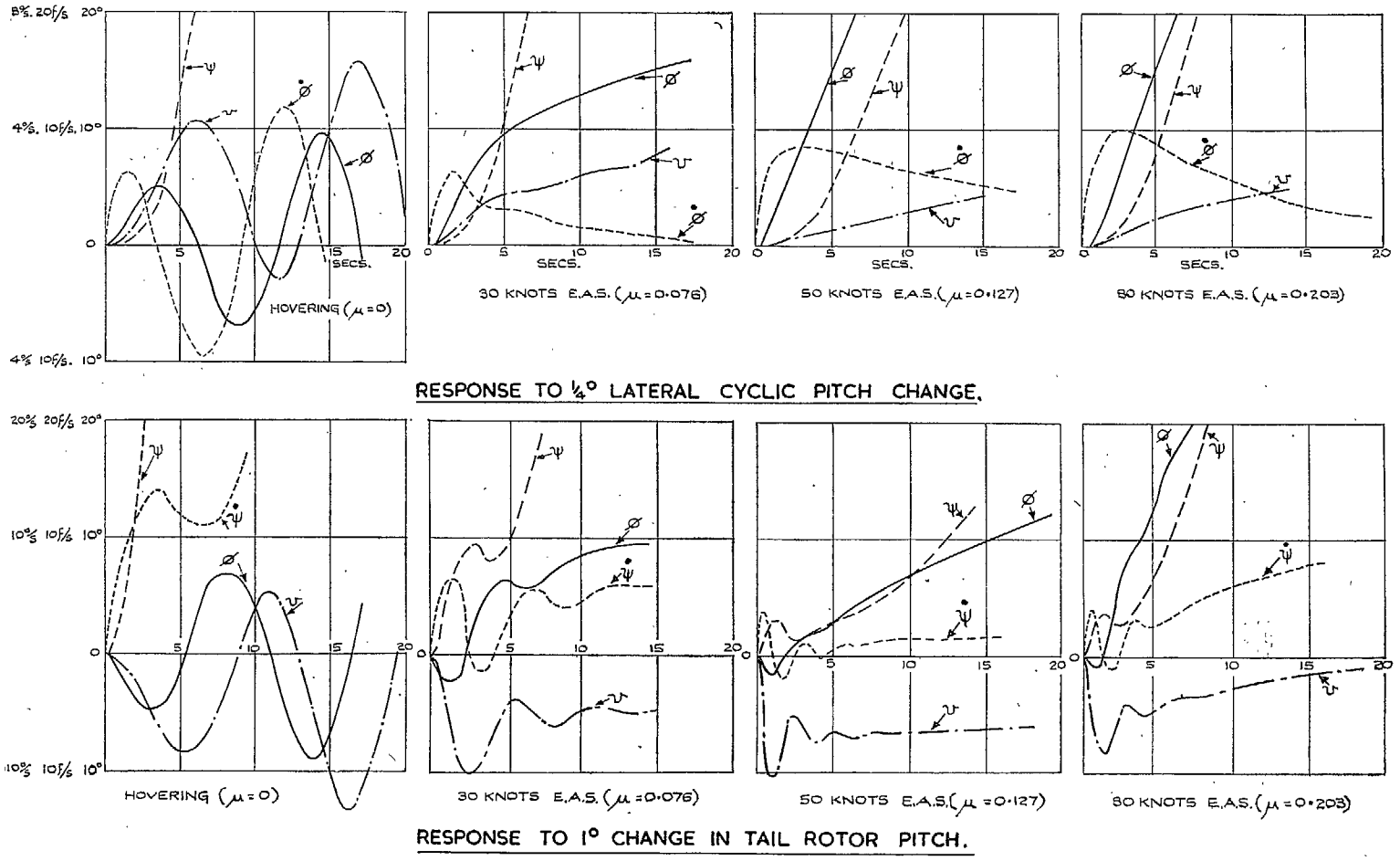

FIG. 9. *Sycamore* at 2000 ft I.C.A.N. Theoretical response to controls.

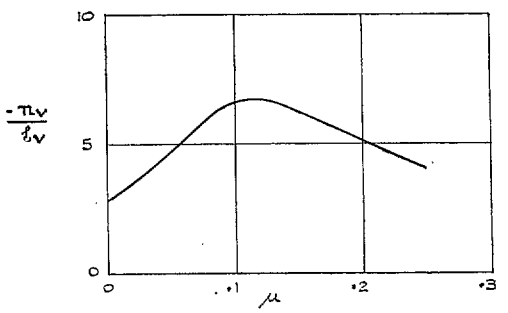

FIG. 10. Ratio n_v/l_v for *Sycamore* at 2000 ft I.C.A.N.

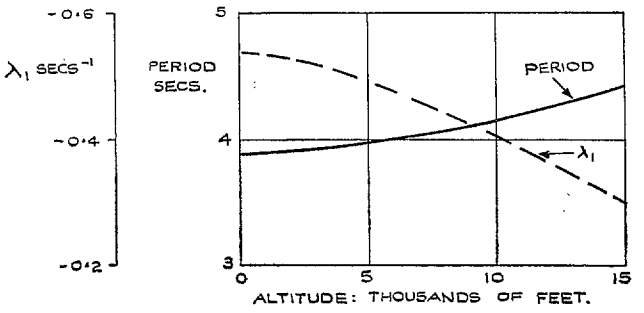

FIG. 11. Effect of altitude on period and damping of lateral oscillation of *Sycamore* at $\mu = 0{\cdot}15$.

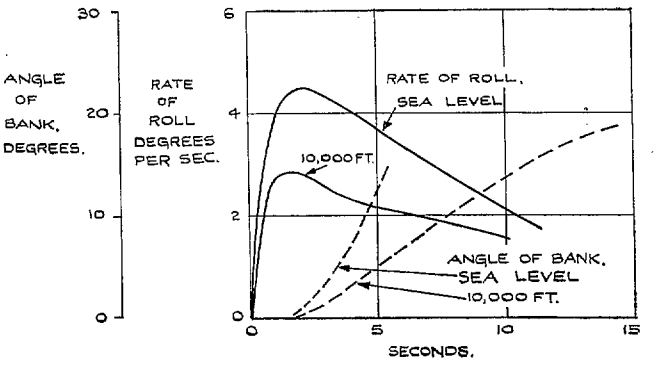

FIG. 12. Response of *Sycamore* to $\frac{1}{4}$ deg change in lateral cyclic stick at sea level and 10,000 ft I.C.A.N. ($\mu = 0{\cdot}15$).

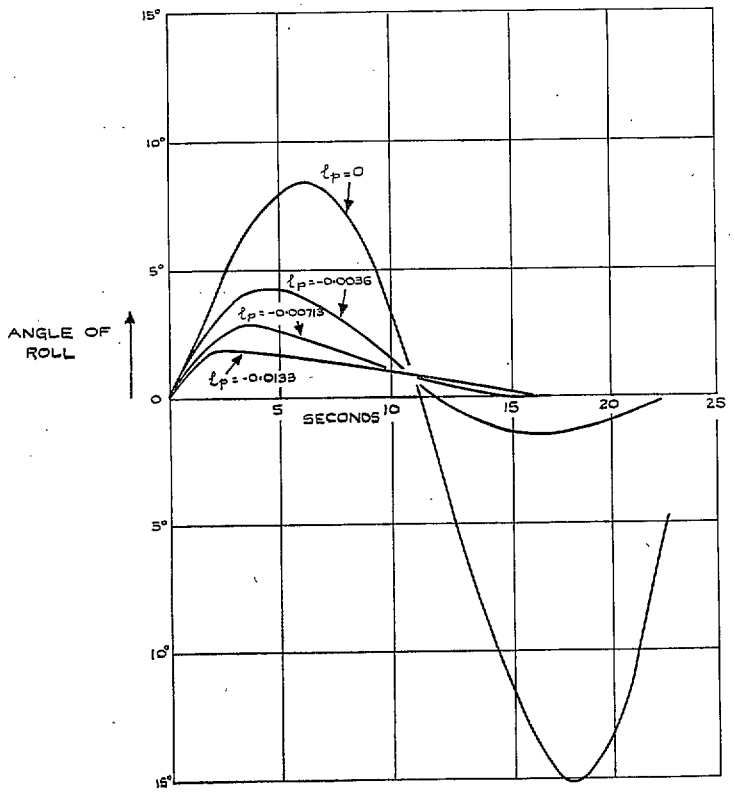

FIG. 13. Response of *Sycamore* to a rolling disturbance at $\mu = 0{\cdot}25$ with various values of l_p.

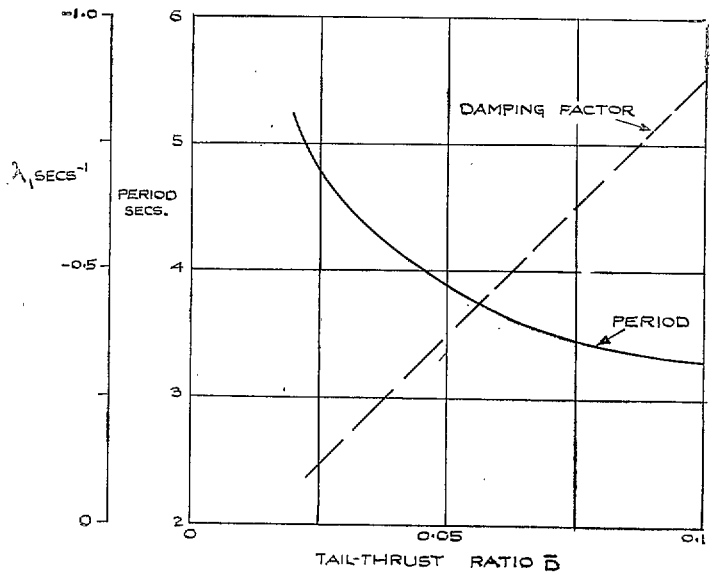

FIG. 14. Effect of change of tail thrust ratio on period and damping of lateral-directional oscillation at $\mu = 0{\cdot}15$.

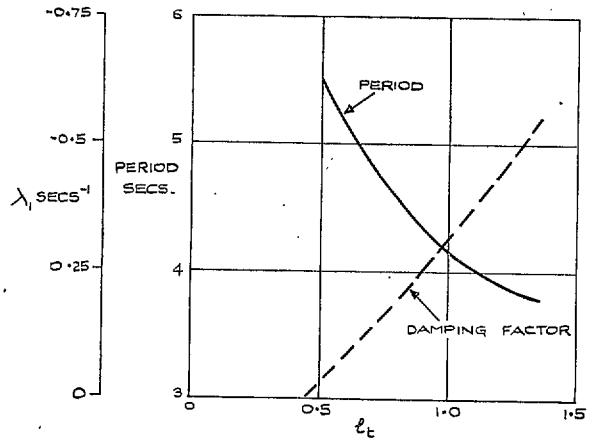

FIG. 15. Effect of change of l_t on period and damping of lateral-directional oscillation at $\mu = 0{\cdot}15$.

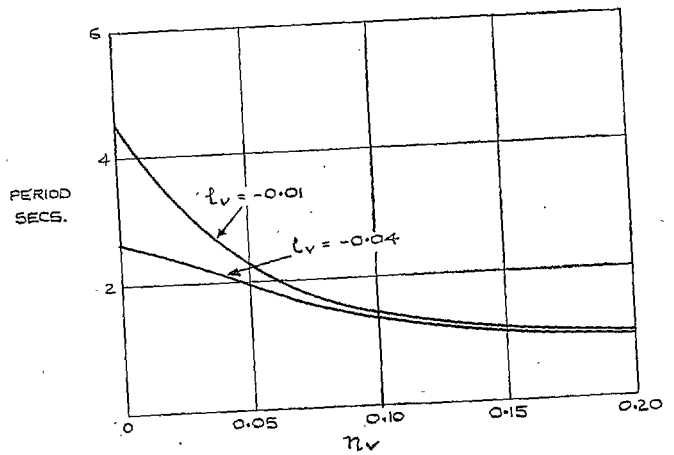

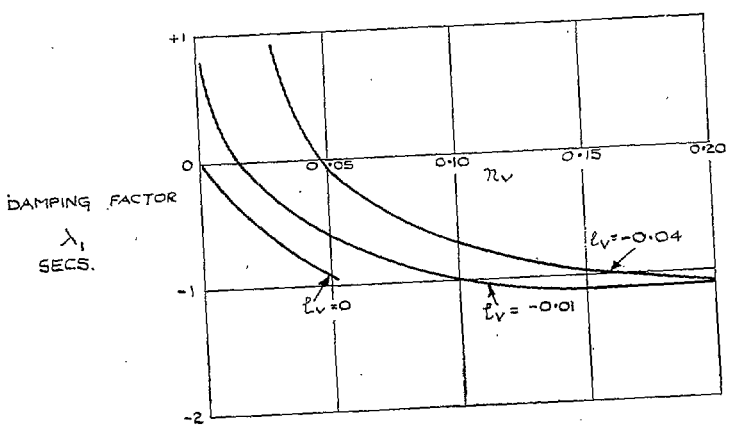

FIG. 16. Effect of changes in l_v and n_v on period and damping of lateral-directional oscillation at $\mu = 0{\cdot}15$.

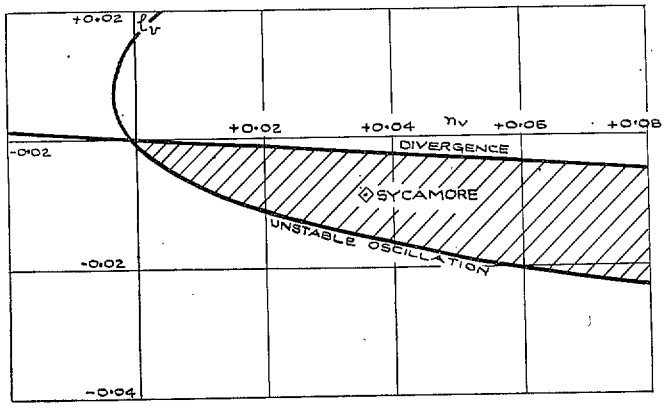

(a) $\mu = 0{\cdot}05$

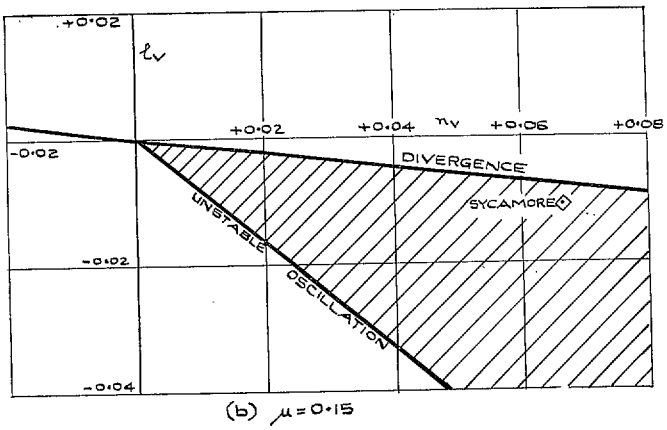

(b) $\mu = 0{\cdot}15$

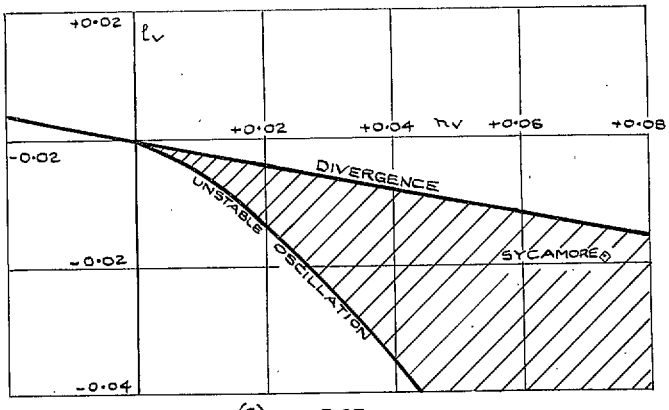

(c) $\mu = 0{\cdot}25$

FIG. 17. Effect of changes of l_v and n_v on stability. Boundaries for $\mu = 0{\cdot}05$, $0{\cdot}15$ and $0{\cdot}25$.

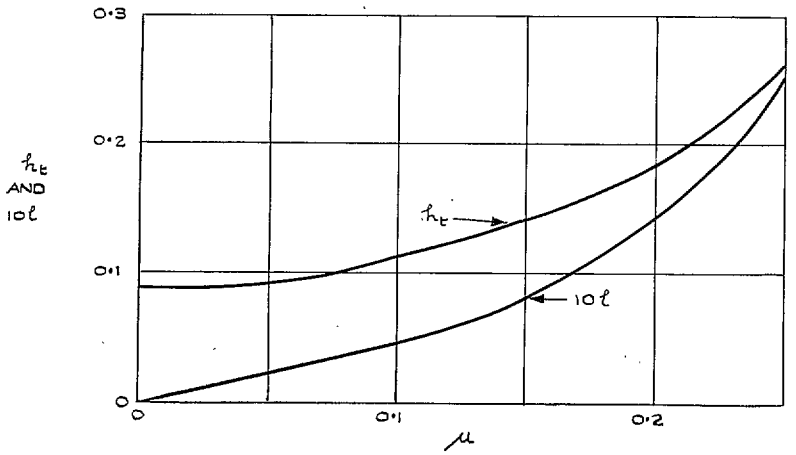

FIG. 18. h_t and l for a *Sycamore*. Experimental results.

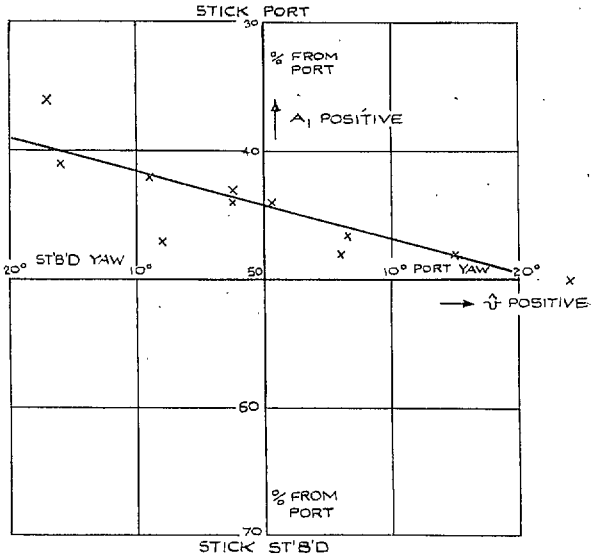

LATERAL STICK POSITION v YAW ANGLE.

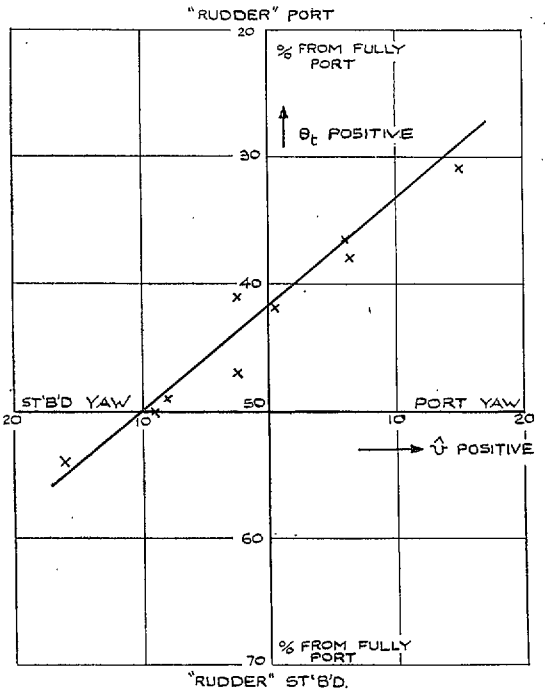

FIG. 19. Control positions in steady yawed flight.

(78655) Wt. 54/8210 K.5 12/60 Hw.

Publications of the Aeronautical Research Council

ANNUAL TECHNICAL REPORTS OF THE AERONAUTICAL RESEARCH COUNCIL (BOUND VOLUMES)

1941 Aero and Hydrodynamics, Aerofoils, Airscrews, Engines, Flutter, Stability and Control, Structures. 63*s.* (post 2*s.* 3*d.*)

1942 Vol. I. Aero and Hydrodynamics, Aerofoils, Airscrews, Engines. 75*s.* (post 2*s.* 3*d.*)
Vol. II. Noise, Parachutes, Stability and Control, Structures, Vibration, Wind Tunnels. 47*s.* 6*d.* (post 1*s.* 9*d.*)

1943 Vol. I. Aerodynamics, Aerofoils, Airscrews. 80*s.* (post 2*s.*)
Vol. II. Engines, Flutter, Materials, Parachutes, Performance, Stability and Control, Structures. 90*s.* (post 2*s.* 3*d.*)

1944 Vol. I. Aero and Hydrodynamics, Aerofoils, Aircraft, Airscrews, Controls. 84*s.* (post 2*s.* 6*d.*)
Vol. II. Flutter and Vibration, Materials, Miscellaneous, Navigation, Parachutes, Performance, Plates and Panels, Stability, Structures, Test Equipment, Wind Tunnels. 84*s.* (post 2*s.* 6*d.*)

1945 Vol. I. Aero and Hydrodynamics, Aerofoils. 130*s.* (post 3*s.*)
Vol. II. Aircraft, Airscrews, Controls. 130*s.* (post 3*s.*)
Vol. III. Flutter and Vibration, Instruments, Miscellaneous, Parachutes, Plates and Panels, Propulsion. 130*s.* (post 2*s.* 9*d.*)
Vol. IV. Stability, Structures, Wind Tunnels, Wind Tunnel Technique. 130*s.* (post 2*s.* 9*d.*)

1946 Vol. I. Accidents, Aerodynamics, Aerofoils and Hydrofoils. 168*s.* (post 3*s.* 3*d.*)
Vol. II. Airscrews, Cabin Cooling, Chemical Hazards, Controls, Flames, Flutter, Helicopters, Instruments and Instrumentation, Interference, Jets, Miscellaneous, Parachutes. 168s. (post 2*s.* 9*d.*)

1947 Vol. I. Aerodynamics, Aerofoils, Aircraft. 168*s.* (post 3*s.* 3*d.*)
Vol. II. Airscrews and Rotors, Controls, Flutter, Materials, Miscellaneous, Parachutes, Propulsion, Seaplanes, Stability, Structures, Take-off and Landing. 168*s.* (post 3*s.* 3*d.*)

Special Volumes

Vol. I. Aero and Hydrodynamics, Aerofoils, Controls, Flutter, Kites, Parachutes, Performance, Propulsion, Stability. 126*s.* (post 2*s.* 6*d.*)

Vol. II. Aero and Hydrodynamics, Aerofoils, Airscrews, Controls, Flutter, Materials, Miscellaneous, Parachutes, Propulsion, Stability, Structures. 147*s.* (post 2*s.* 6*d.*)

Vol. III. Aero and Hydrodynamics, Aerofoils, Airscrews, Controls, Flutter, Kites, Miscellaneous, Parachutes, Propulsion, Seaplanes, Stability, Structures, Test Equipment. 189*s.* (post 3*s.* 3*d.*)

Reviews of the Aeronautical Research Council

1939–48 3*s.* (post 5*d.*) 1949–54 5*s.* (post 5*d.*)

Index to all Reports and Memoranda published in the Annual Technical Reports

1909–1947 R. & M. 2600 6*s.* (post 2*d.*)

Indexes to the Reports and Memoranda of the Aeronautical Research Council

Between Nos. 2351–2449	R. & M. No. 2450 2*s.* (post 2*d.*)
Between Nos. 2451–2549	R. & M. No. 2550 2*s.* 6*d.* (post 2*d.*)
Between Nos. 2551–2649	R. & M. No. 2650 2*s.* 6*d.* (post 2*d.*)
Between Nos. 2651–2749	R. & M. No. 2750 2*s.* 6*d.* (post 2*d.*)
Between Nos. 2751–2849	R. & M. No. 2850 2*s.* 6*d.* (post 2*d.*)
Between Nos. 2851–2949	R. & M. No. 2950 3*s.* (post 2*d.*)

HER MAJESTY'S STATIONERY OFFICE

from the addresses overleaf

Printed and published by
HER MAJESTY'S STATIONERY OFFICE

To be purchased from
York House, Kingsway, London W.C.2
423 Oxford Street, London W.1
13A Castle Street, Edinburgh 2
109 St. Mary Street, Cardiff
39 King Street, Manchester 2
50 Fairfax Street, Bristol 1
2 Edmund Street, Birmingham 3
80 Chichester Street, Belfast 1
or through any bookseller

Printed in England

R. & M. No. 3149

S.O. Code No. 23-3149